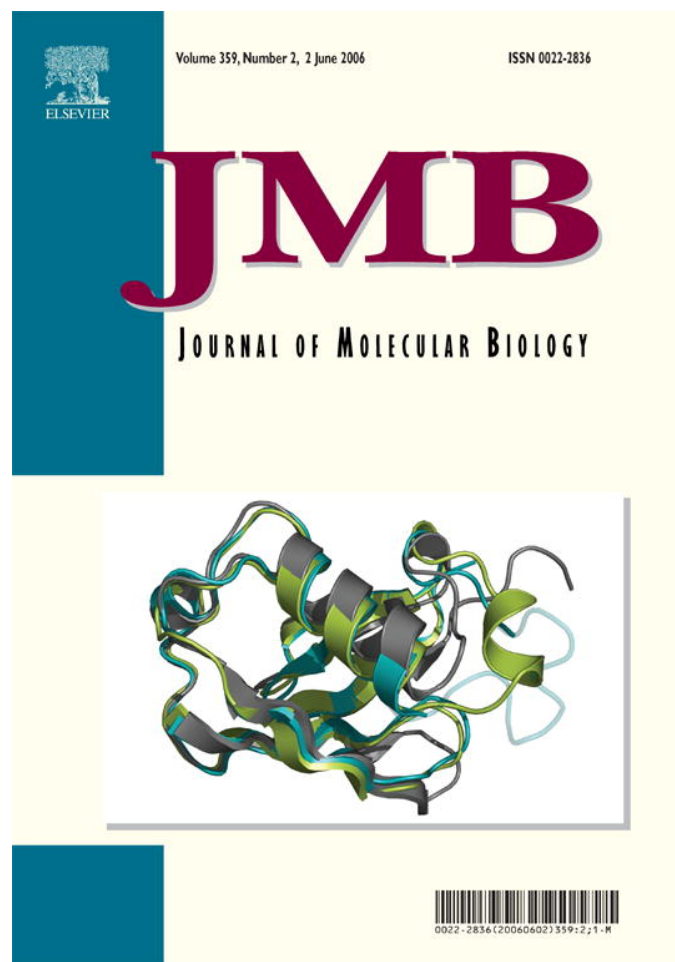


Provided for non-commercial research and educational use only.  
Not for reproduction or distribution or commercial use.



This article was originally published in a journal published by Elsevier, and the attached copy is provided by Elsevier for the author's benefit and for the benefit of the author's institution, for non-commercial research and educational use including without limitation use in instruction at your institution, sending it to specific colleagues that you know, and providing a copy to your institution's administrator.

All other uses, reproduction and distribution, including without limitation commercial reprints, selling or licensing copies or access, or posting on open internet sites, your personal or institution's website or repository, are prohibited. For exceptions, permission may be sought for such use through Elsevier's permissions site at:

<http://www.elsevier.com/locate/permissionusematerial>

## Unique Regulation of the Active site of the Serine Esterase S-Formylglutathione Hydrolase

Ian Cummins<sup>1†</sup>, Katherine McAuley<sup>2†</sup>, Anthony Fordham-Skelton<sup>3</sup>  
Ralf Schworer<sup>4</sup>, Patrick G. Steel<sup>5</sup>, Benjamin G. Davis<sup>4</sup>  
and Robert Edwards<sup>1\*</sup>

<sup>1</sup>Centre for Bioactive Chemistry  
and School of Biological and  
Biomedical Sciences, University  
of Durham, Durham  
DH1 3LE, UK

<sup>2</sup>Diamond Light Source Ltd  
Diamond House, Chilton  
Didcot, Oxfordshire  
OX11 0DE, UK

<sup>3</sup>CLRC Daresbury, Warrington  
WA4 4AD, UK

<sup>4</sup>Department of Chemistry  
University of Oxford, Chemistry  
Research Laboratory, Mansfield  
Road, Oxford OX1 3TA, UK

<sup>5</sup>Department of Chemistry  
University of Durham, Durham  
DH1 3LE, UK

S-Formylglutathione hydrolases (SFGHs) are highly conserved thioesterases present in prokaryotes and eukaryotes, and form part of the formaldehyde detoxification pathway, as well as functioning as xenobiotic-hydrolysing carboxyesterases. As defined by their sensitivity to covalent modification, SFGHs behave as cysteine hydrolases, being inactivated by thiol alkylating agents, while being insensitive to inhibition by organophosphates such as paraoxon. As such, the enzyme has been classified as an esterase D in animals, plants and microbes. While SFGHs do contain a conserved cysteine residue that has been implicated in catalysis, sequence analysis also reveals the classic catalytic triad of a serine hydrolase. Using a combination of selective protein modification and X-ray crystallography, *At*SFGH from *Arabidopsis thaliana* has been shown to be a serine hydrolase rather than a cysteine hydrolase. Uniquely, the conserved reactive cysteine (Cys59) previously implicated in catalysis lies in close proximity to the serine hydrolase triad, serving a gate-keeping function in comprehensively regulating access to the active site. Thus, any covalent modification of Cys59 inhibited all hydrolase activities of the enzyme. When isolated from *Escherichia coli*, a major proportion of recombinant *At*SFGH was recovered with the Cys59 forming a mixed disulfide with glutathione. Reversible disulfide formation with glutathione could be demonstrated to regulate hydrolase activity *in vitro*. The importance of Cys59 in regulating *At*SFGH *in planta* was demonstrated in transient expression assays in *Arabidopsis* protoplasts. As determined by fluorescence microscopy, the Cys59Ser mutant enzyme was shown to rapidly hydrolyse 4-methylumbelliferyl acetate in paraoxon-treated cells, while the native enzyme was found to be inactive. Our results clarify the classification of *At*SFGHs as hydrolases and suggest that the regulatory and conserved cysteine provides an unusual redox-sensitive regulation to an enzyme functioning in both primary and xenobiotic metabolism in prokaryotes and eukaryotes.

© 2006 Elsevier Ltd. All rights reserved.

**Keywords:** *Arabidopsis thaliana*; esterase D; formaldehyde detoxification; S-glutathionylation; thioesterase

\*Corresponding author

† I.C. and K.M. contributed equally to this work.  
Abbreviations used: ESI TOF MS, electrospray ionization time-of-flight mass spectrometry; MUA, 4-methylumbelliferyl acetate; SFGH, S-formylglutathione hydrolase; pNPA, p-nitrophenylacetate; S-AG, S-acetylglutathione; FP-biotin, 10-(fluoroethoxyphosphinyl)-N-(biotinamidopentyl)decanamide; MTS, methylthio-sulfonate.

E-mail address of the corresponding author:  
robert.edwards@durham.ac.uk

### Introduction

While relatively well characterised in animals and microorganisms, the non-specific carboxyesterases of plants have only recently come to light as proteins with essential and diverse roles in signalling and defence against pathogens,<sup>1</sup> and the metabolism of secondary metabolites<sup>2</sup> and herbicides.<sup>3</sup> On the basis of genome annotation, esterase D was the first carboxyesterase active in hydrolysing model xenobiotic esters identified in *Arabidopsis*

*thaliana*. Esterase D, originally identified as a carboxyesterase in man with high activity toward 4-methylumbelliferyl acetate (MUA), was subsequently shown to be S-formylglutathione hydrolase (SFGH, EC 3.1.1.56), an enzyme catalysing the hydrolysis of S-formylglutathione to formic acid and glutathione.<sup>4</sup> SFGH is part of a pathway of formaldehyde detoxification conserved in prokaryotes and eukaryotes,<sup>5</sup> with the enzyme functionally characterised in *Paracoccus denitrificans*,<sup>6</sup> *Saccharomyces cerevisiae*,<sup>7</sup> *Candida boidinii*,<sup>8</sup> *Escherichia coli*<sup>9</sup> and *A. thaliana*.<sup>10,11</sup> Searches for homologues in other genome and EST databases show remarkable conservation in the sequence of SFGHs. In each case, the enzyme has been described as having an essential catalytic cysteine residue based on inhibition studies with sulfhydryl-modifying agents. In support of this, SFGHs are insensitive to organophosphate insecticides, which are selective inactivating agents of serine hydrolases.<sup>10</sup>

Alignments of the sequences of SFGHs from different species show the presence of a conserved cysteine residue (Cys59 in *Arabidopsis*; Figure 1), which has been suggested to be the catalytic residue.<sup>11</sup> However, a further study of the sequence reveals the presence of a conserved serine esterase catalytic motif (GHSMGG), together with the aspartate and histidine residues required to complete a putative serine hydrolase catalytic triad (Figure 1). Informatics would therefore suggest that SFGH was actually a serine hydrolase, even though the inhibition characteristics of the enzyme are those of a cysteine hydrolase.

In view of the growing realisation of the functional importance of carboxyesterases in plant physiology and metabolism, as well as unravelling the classification and mechanism of catalysis of the

highly conserved SFGHs, it was of interest to dissect the enzyme chemistry of the respective enzyme recently cloned from *Arabidopsis* (*AtSFGH*).<sup>10,11</sup> This functional characterisation has been achieved by a combination of solving the crystal structure of *AtSFGH*, selective covalent modification and site-directed mutagenesis. A technical account of the crystallisation of the recombinant *Arabidopsis* SFGH has been reported.<sup>12</sup>

## Results

### Selective covalent modification of *AtSFGH* with inhibitors

His-tagged *AtSFGH* was purified from *E. coli* lysates by Ni chelate affinity chromatography and treated with DTT to ensure that all free cysteine molecules present were fully reduced. Using electrospray ionization time-of-flight mass spectrometry (ESI TOF MS), a dominant polypeptide (32,586 Da) was observed, corresponding to the predicted mass of *AtSFGH* (Table 1). *AtSFGH* was exposed to S-alkylating agents and specific inhibitors of serine hydrolases, and the effect on carboxyesterase and thioesterase enzyme activity was determined using *p*-nitrophenylacetate (pNPA) and S-acetylglutathione (S-AG), respectively, as substrates. S-AG was used as the glutathione thioester substrate, as S-formylglutathione undergoes rapid non-enzymic hydrolysis, which interfered with the assays.<sup>10</sup> The effect of the chemical treatments on the mass of *AtSFGH* was also monitored by ESI TOF MS. *AtSFGH* was inhibited when exposed to the S-alkylating agents iodoacetamide and N-ethylmaleimide. As determined by

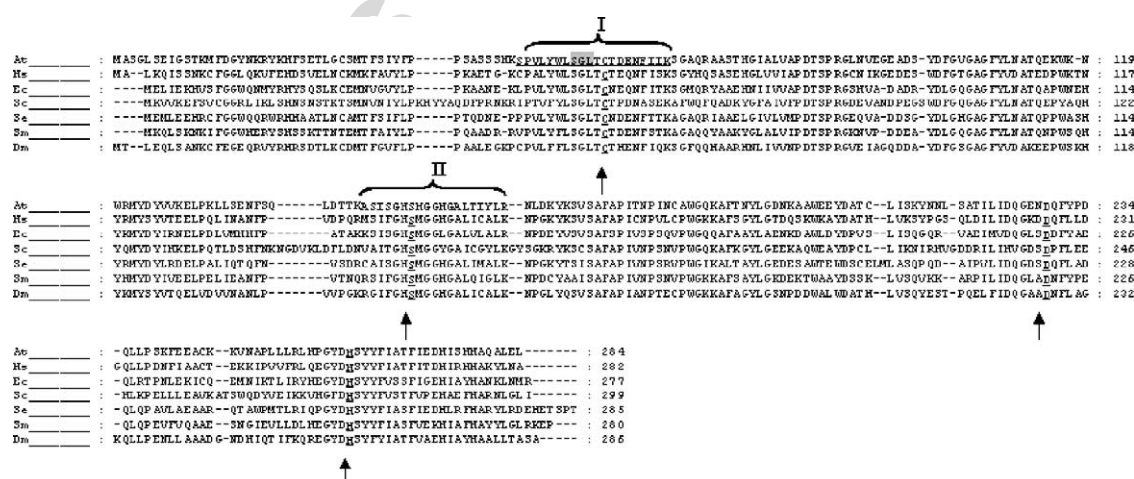


**Figure 1.** Alignments of predicted amino acid sequences of SFGHs from *Arabidopsis thaliana* (At), *Homo sapiens* (Hs), *Escherichia coli* (Ec), *Saccharomyces cerevisiae* (Sc), *Synechococcus elongatus* (Se), *Streptococcus mutans* (Sm) and *Drosophila melanogaster* (Dm). The conserved cysteine residues and the individual residues contributing to the catalytic serine triad are shown in bold and underlined. The oxyanion hole motif is highlighted. The tryptic fragments of *AtSFGH* containing the conserved cysteine (I) and serine (II), which underwent selective covalent modification, are underlined. As determined by ESI-TOF-MS after deconvolution the molecular masses of peptide I were 2299.6 Da (native); predicted 2299.6 Da) 2357.6 Da (plus acetamide; predicted 2357.6 Da), 2607.0 Da, (plus glutathione; predicted 2604.6 Da). For peptide II 1928.2 Da (native; predicted 1928.2 Da); 2501.2 Da (plus phosphonobiotin; predicted 2501.2 Da).

**Table 1.** Effect of covalent modification by chemical derivatisation or mutagenesis on the hydrolase activity and mass of recombinant *AtSFGH*

| DTT +/– | Chemical modification                                     | Polypeptide mass (Da) (abundance %) | Enzyme activity |       |
|---------|---|-------------------------------------|-----------------|-------|
|         |   |                                     | <i>p</i> NPA    | S-AG  |
| +       | Wild-type   | 32,586 (100)                        | 62.1            | 124.2 |
| +       | Iodoacetamide (1 mM)                                      | 32,586 (58), +58 (42)               | 34.6            | 68.0  |
| +       | <i>N</i> -Ethylmaleimide (1 mM)                           | +627 (100)                          | 0               | 0     |
| +       | Paraoxon (1 mM)   | 32,588 (100)                        | 61.3            | 122.6 |
| +       | PMSF (1 Mm)   | 32,588 (100)                        | 60.5            | 122.9 |
| +       | FP-biotin (20 $\mu$ M)                                    | 32,584 (51), +306 (16), +575 (34)   | 29.4            | 55.6  |
| +       | Iodoacetamide (10 mM)/FP-biotin (20 $\mu$ M) <sup>a</sup> | +58 (84), +114 (16)                 | 0               | 0     |
| +       | GSSG (2 mM)   | 32,583 (62), +303 (38)              | 40.1            | 72.5  |
| +       | Cys59Ser + GSSG (2 mM)                                    | 32,574 (100)                        | 63.8            | 122.4 |
| +       | Ser152Ala   | 32,574 (100)                        | 0               | 0     |
| –       | Wild-type, no modification                                | 32,586 (88), +303 (12)              | 59.5            | 118.3 |
| –       | Cys59Ser  | 32,574 (100)                        | 65.3            | 125.8 |

Protein (20  $\mu$ M) was fully reduced with 2 mM DTT before chemical treatment unless specified otherwise. Carboxyesterase and thioesterase activity was determined using *p*NPA and S-AG as substrate, respectively. In each case, the masses of the additions to the *AtSFGH* polypeptide (native mass 32,586 Da) derived from the chemical treatments are given, together with the relative abundance of the respective ionisable species.

<sup>a</sup> Sequential chemical treatments.

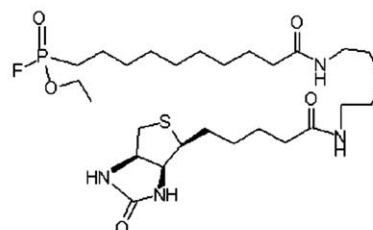
MS, treatment with iodoacetamide resulted in the partial alkylation of the SFGH pool at a single site, which caused a directly proportional decline in both carboxyesterase and thioesterase activity. *N*-Ethylmaleimide abolished all activity and resulted in *AtSFGH* undergoing an increase in mass of 627 Da, representing five maleimidyl additions to all the available cysteine residues in the protein. Tryptic digestion of the singly modified *AtSFGH* derived from treatment with iodoacetamide resulted in the identification of a peptide that perfectly matched the predicted mass of the fragment (SPVLYWLSGLTCTDENFIIK) after allowing for the modification of the only cysteine residue (Cys59) present (Figure 1). This confirmed that covalent modification of the conserved Cys59 resulted in a proportional loss of hydrolase activities. Treatment of *AtSFGH* with the organophosphate insecticide *O,O*-diethyl-*O*-*p*-nitrophenylphosphoric acid (paraoxon), which is a potent inhibitor of plant serine carboxyesterases<sup>3</sup> and phenylmethylsulfonyl fluoride (PMSF), a classic inhibitor of serine hydrolases, had no effect on enzyme activities or the mass of the protein. In addition to these conventional serine hydrolase inhibitors, a custom-synthesised inhibitor, 10-(fluoroethoxyphosphinyl)-*N*-(biotinamidopentyl)decanamide (FP-biotin) (Figure 2) was also used. FP-biotin has been shown to be a powerful *in vitro* inhibitor of serine hydrolases in both animals<sup>13</sup> and plants,<sup>3</sup> being able to selectively acylate the active site residues of a diverse range of enzymes. Treatment of *AtSFGH* with equimolar quantities of FP-biotin strongly inhibited the hydrolysis of both *p*-NPA and S-AG. This was associated with 40% of the protein showing an increased mass of 573 Da, consistent with its single covalent modification with the biotinylated probe after correcting for the loss of the displaced fluorine atom. Following tryptic digestion, acylation was shown to have occurred

within the peptide fragment ASIAGHSMGGH-GALTIYLR (Figure 1), indicating that one of the two serine residues present had been labelled due to its catalytic activity.

#### FP-biotin

(mass increase = 573)

(a)



#### MTS reagents

R = SO<sub>2</sub>CH<sub>3</sub>

(b)

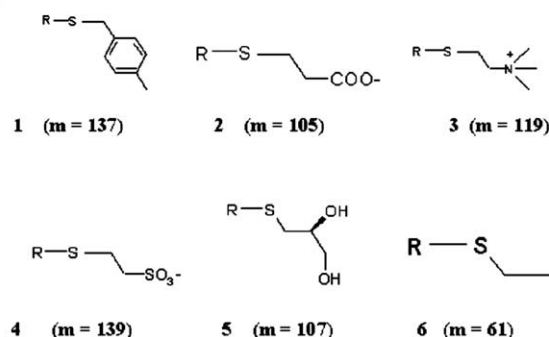


**Figure 2.** Chemical reagents used to selectively modify (a) Ser152 using fluorophosphonobiotin and (b) Cys59 using a series of MTS reagents. In each case, native SFGH (32586 Da) underwent the mass increase shown in parentheses. With the MTS reagents, all the *AtSFGH* underwent derivatisation to the respective disulfide resulting in a loss of all activity.

The studies with FP-biotin demonstrated that the putative serine catalytic site was indeed active. To investigate the chemical connectivity between Cys59 and the catalytic serine residue, sequential labelling studies were carried out with FP-biotin and iodoacetamide. Interestingly, while the prior modification of *AtSFGH* with FP-biotin did not affect subsequent alkylation of Cys59, the covalent modification of *AtSFGH* with FP-biotin could be prevented if the protein was first treated with iodoacetamide (Table 1).

### Structural biology of *AtSFGH*; identification of a serine hydrolase catalytic triad and location of the regulatory Cys29

To reconcile the roles of the serine and Cys59 residues within the putative active site, *AtSFGH* was crystallised and its three-dimensional structure determined in space group C2 at a resolution of 1.7 Å ( $R$ -factor of 18.4% and  $R_{\text{free}}$  21.5%). Analysis of the model with PROCHECK<sup>14</sup> and WHAT\_CHECK,<sup>15</sup> showed good stereochemistry, with only the catalytic serine residues in the disallowed region of the Ramachandran plot. Three molecules were determined in the asymmetric unit, denoted A, B and C, giving a total of 850 amino acid residues and 547 water molecules in the final model.

In terms of overall structure, each protein molecule consisted of a central  $\beta$ -sheet surrounded by  $\alpha$  helices, typical of the  $\alpha/\beta$  hydrolase fold. The  $\beta$ -sheet was comprised of nine, mostly parallel  $\beta$ -strands in the order  $\beta$ -A,  $\beta$ -B,  $\beta$ -C,  $\beta$ -E,  $\beta$ -D,  $\beta$ -F,  $\beta$ -G,  $\beta$ -H and  $\beta$ -I (Figure 3(a)). Strands  $\beta$ -A and  $\beta$ -C were anti-parallel to the other  $\beta$ -strands. Surrounding the  $\beta$ -sheet core were eight  $\alpha$  helices and three  $3_{10}$  helices. *AtSFGH* had a stretch of 35 residues (85–120) with no secondary structure elements except for a short  $3_{10}$  helix (residues 114–116). There was clear experimental electron density for this region in molecule A, but it was less well defined in molecule B and was almost completely missing for these residues in molecule C. Since most of this part of the polypeptide chain protrudes from the protein, the poor electron density in this region indicates that the loop is flexible.

Gel-filtration experiments<sup>10</sup> and light-scattering studies had demonstrated that *AtSFGH* is a dimeric protein. The crystal structure had three molecules per asymmetric unit, but closer inspection showed that dimers were formed between molecules B and C, and between one molecule A and a symmetry-related molecule A. The dimer association was mainly hydrophobic in character, with 61% of the interface residues being non-polar (Protein-Protein Interaction Server<sup>†</sup>), with a buried surface area of 847 Å<sup>2</sup>. However, there were also six inter-dimer hydrogen bonds between residues Asp B/C 15 N-Tyr C/B 260 OH, Lys B/C 12 NZ-Pro C/B 258 O,

Phe B/C 14 N-Thr C/B 269 OG1. The positioning of Met14 in the interface region between the two molecules of the dimer helped explain why its replacement with selenomethionine led to observable differences in packing of the crystal lattice under pressure.<sup>12</sup> Thus, native crystals can be induced to change space group to  $P3_121$  when subjected to pressure, whereas the selenomethionine-labelled crystals could not undergo the same transformation.

The overall structure of the *AtSFGH* dimer is shown in Figure 3(b), with the active site of the enzyme consisting of residues Ser152, His262 and Asp229 arranged as the classic catalytic triad of an  $\alpha/\beta$  hydrolase (Figure 3(c)). Thus, Ser152 was located as a nucleophilic "elbow" on the sharp turn between strand  $\beta$ -F and helix  $\alpha$ -4, with this strained geometry typical of the catalytic serine in this family of enzymes. The hydrogen bonding distances between Ser152 OH–His262 NE2 = 2.9 Å and Asp229 OD2–His262 ND1 = 2.5 Å were also perfectly arrayed for a catalytic triad. Overall, the active site cleft had approximate dimensions of 12 Å long by 8 Å wide and 8 Å deep, with the "regulatory" Cys59 sited on the edge of the cleft, above and approximately 9 Å away from Ser152.

Attempts to co-crystallise *AtSFGH* with thioester or carboxyester substrates were unsuccessful. However, X-ray diffraction data were derived for *AtSFGH* complexed with the thioesterase reaction product glutathione. Crystallographic data were collected to a resolution of 2.14 Å with an  $R$ -factor of 17.6% and an  $R_{\text{free}}$  of 22.3%. Following molecular replacement and several refinement cycles, the electron density maps were inspected and a region of positive difference density identified as a molecule of glutathione in the active site of *AtSFGH* (Figure 4(a)). While the Gly and the Cys residues of glutathione could be seen clearly in the electron density maps, the  $\gamma$ -Glu residue was less well ordered. As shown in Figure 4(b), glutathione interacted with *AtSFGH* through a salt-bridge between the carboxylate group of the Gly residue and a conserved Lys67 of *AtSFGH* (distance = 2.3 Å). There was also a hydrogen bond between the carboxylate group of the Glu of glutathione and Gln230 N. Cys59 was not involved directly in the binding of glutathione to *AtSFGH*, but its sulfur atom is only 3.8 Å from the Gly residue of the tripeptide. While the co-crystallisation of glutathione with *AtSFGH* gave useful insights into the likely orientation of binding of the respective thioesters, it was clear that the actual substrates must dock deeper into the site. Thus, the sulfur atom of glutathione was estimated to be 6.8 Å away from the hydroxyl group of Ser152. Since the glutathione thioester substrate must approach closer to Ser152 than this for catalysis to occur, it must be assumed that the product-enzyme interaction observed here is subtly different from that seen when the substrate binds to the active site.

<sup>†</sup> <http://www.biochem.ucl.ac.uk/bsm/PP/server>

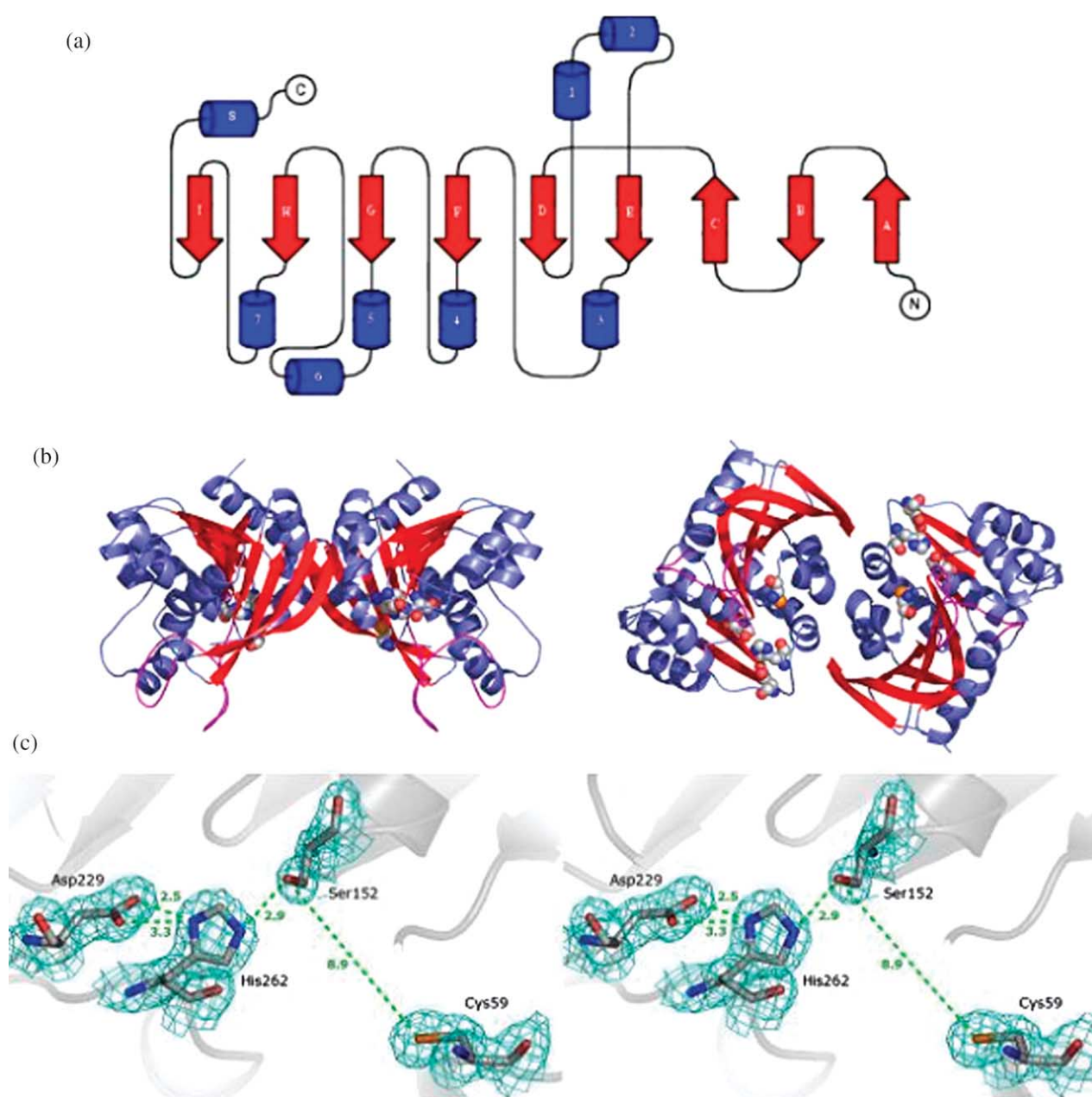


**Figure 3.** Crystal structure of *AtSFGH*. (a) Topology diagram of *SFGH* with helices represented by blue cylinders and strands by red arrows. (b) Two views, related by a  $90^\circ$   $x$ -rotation, of the structure of the *AtSFGH* dimer, with colouring scheme as above. The active site residues are represented as spheres. The flexible loop region is shown in magenta (Figures 4(b) and (c), and 5; PyMol<sup>34</sup>). (c) Close-up of the active site of *AtSFGH*. The active site residues are Ser152, Asp229 and His262. Also shown is Cys59. The distances in green indicate the hydrogen bonds between residues of the catalytic triad. The distance in yellow (8.8 Å) is between Ser152 OH and Cys59.

### Selective mutation and modification of Cys59 and Ser152.

Through a combination of protein modification studies and structural biology it was possible to identify both Cys59 and Ser152 as critical residues in regulating catalysis in *AtSFGH*. Using site-directed mutagenesis, Ser152Ala (S152A) and Cys59Ser (C59S) mutant enzymes were generated, assayed for activity and their sensitivity to chemical regulation determined, as compared with the

wild-type enzyme. The S152A mutant was unable to hydrolyse either *p*-NP or *S*-AG. In contrast, the C59S mutant showed indistinguishable activities toward both substrates as compared with freshly reduced wild-type *AtSFGH* (Table 1). This result demonstrated unequivocally that, whereas Ser152 was essential for catalysis, Cys59 was not. Instead, on the basis of its location at the edge of the cleft and proximity to the catalytic triad, it seemed most likely that the observed loss of hydrolase activity upon alkylation of Cys59 was due to the modified

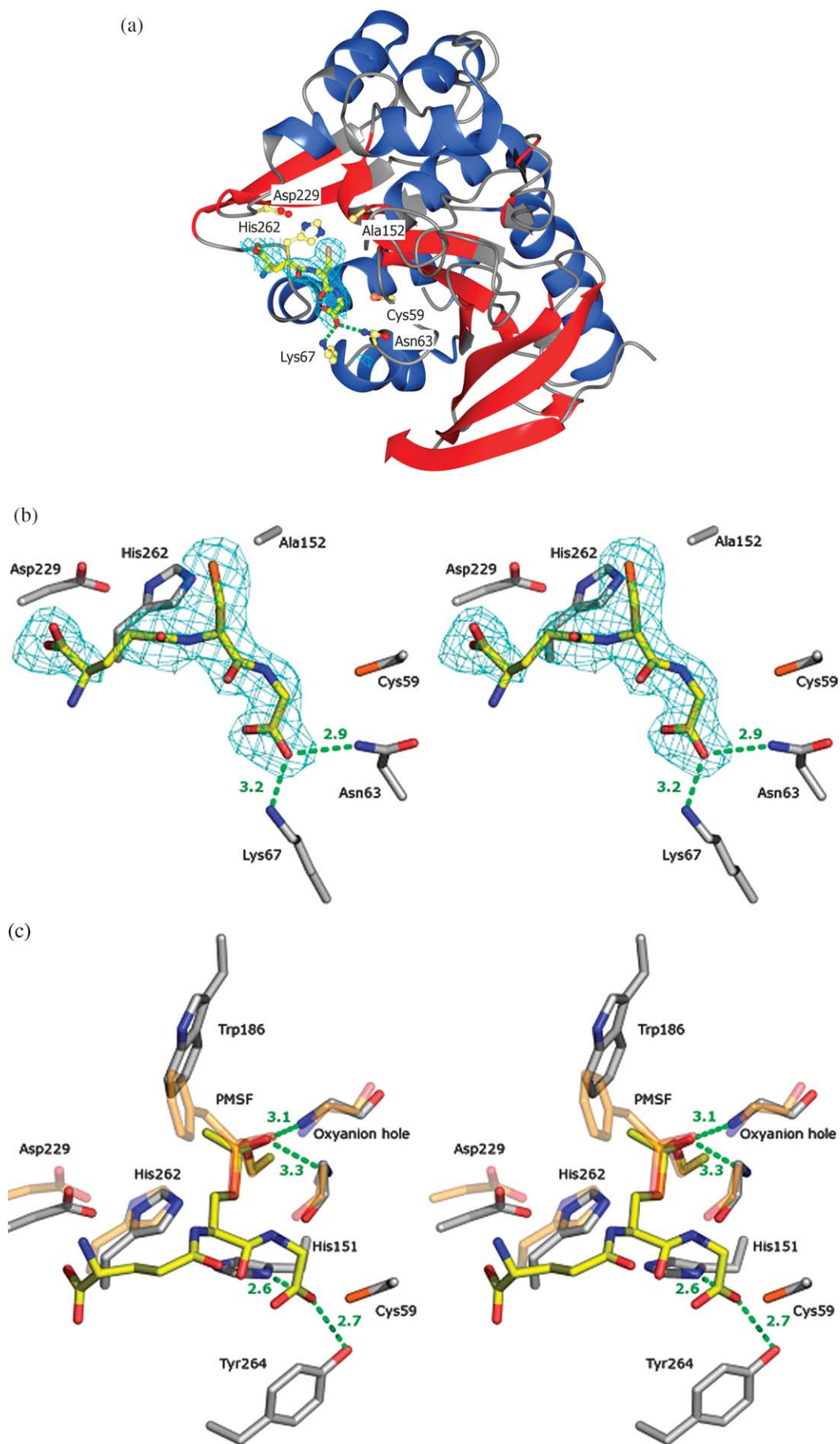


Figure 4. (legend on next page)

residue acting to exclude substrates from the active site. To test this possibility, the Cys59 residue was selectively derivatised with a series of methylthio-sulfonate (MTS) reagents (Figure 2).<sup>16</sup> By carefully controlling the labelling conditions, in each case it was possible to achieve selective mono-derivatisation of the reactive Cys59 residue of the wild-type enzyme as determined by MS. The MTS reagents used represented a series of disulfides (Cys59-SS-R), in which R was varied to display different charge, size and hydrophobic characteristics. Even minor modifications to Cys59 (R=Et) resulted in a total loss of catalytic activity, highlighting the extreme intolerance of the enzyme to modifications in this residue.

### AtSFGH activity is regulated by reversible S-glutathionylation of Cys59

The extreme sensitivity of AtSFGH to inactivation by the MTS reagents suggested that the Cys59 would also undergo disulfide exchange with cellular thiols. In addition, studies with recombinant AtSFGH had consistently shown that the activity of the enzymes was always significantly enhanced by a reducing treatment with DTT,<sup>10</sup> suggesting that Cys59 protein was partially oxidised when originally expressed. Analysis by MS of recombinant AtSFGH isolated from *E. coli* without treatment with DTT showed the presence of two species differing in mass by 305 Da (Table 1). The dominant mass ion corresponded to the native protein, whilst on the basis of our recent studies with recombinant protein tyrosine phosphatases,<sup>17</sup> the larger mass species was most likely a mixed disulfide of AtSFGH and glutathione. The presence of a disulfide was confirmed by treating the protein preparation with DTT, which resulted in the quantitative conversion of the larger mass ion to the parent polypeptide (32,586 Da). The fully reduced AtSFGH was then incubated with oxidised glutathione (GSSG) to promote mixed disulfide formation.<sup>17</sup> Under gentle conditions of thiol exchange (15 min on ice), a single S-glutathionylated derivative of AtSFGH was generated, representing a 38% conversion of parent polypeptide. This was associated with a corresponding decline in carboxyesterase and thioesterase activity (Table 1). Longer incubations with GSSG promoted further S-glutathionylation (data not shown), though this was not associated with any additional loss of activity, confirming that only one cysteine residue of AtSFGH was regulatory. To confirm Cys59 as the critical site for mixed disulfide-mediated inactivation, the singly S-glutathionylated protein was digested with trypsin. As compared with digests of

unmodified AtSFGH, a doubly charged S-glutathionylated derivative of the tryptic fragment SPVLYWLSGLTCTDENFIK (M+2 of 1303.5 Da, compared with a theoretical M+2 of 1303.3 Da) was identified. This unambiguously confirmed Cys59 as the site of selective S-glutathionylation, as well as alkylation. Consistent with this, when the C59S mutant was treated with GSSG under identical conditions, no effect on enzyme activity was determined.

### Cys59 controls the activity of AtSFGH *in vivo*

The chemical modification and mutagenesis studies clearly showed the importance of Cys59 in regulating AtSFGH *in vitro*. To investigate the role of this residue *in vivo*, the coding sequences of the wild-type and C59S mutant enzymes were transiently expressed in *Arabidopsis* protoplasts and the activity of the introduced hydrolase monitored by fluorescence microscopy after feeding the cells with MUA. To monitor the activity of the transgenic AtSFGH, it was first necessary to quench the endogenous esterase activity in the protoplasts. This was achieved by taking advantage of the insensitivity of SFGHs to inhibition by organophosphates, whereas the majority of conventional *Arabidopsis* serine hydrolases are irreversibly inactivated by such a treatment.<sup>10</sup> Transformed protoplasts were pre-treated with the organophosphate paraoxon, and then exposed to MUA. Cells transformed with wild-type AtSFGH showed no MUA hydrolysing activity above background, whereas protoplasts transformed with the C59S mutant enzyme contained many individuals able to hydrolyse the MUA to release the fluorophore (Figure 5).

## Discussion

Using a combination of site-selective covalent modification, structural biology and directed mutagenesis, we have demonstrated that AtSFGH is a classical serine hydrolase whose activity is regulated by Cys59 both *in vivo* and *in vitro*. While roles for cysteine residues in regulating the activity of other serine hydrolases have been described, their action is mediated by quite different mechanisms. Thus, yeast carboxypeptidase Y (EC 3.4.16.5) contains a conserved cysteine residue in the active site, which, when alkylated, inhibits enzyme activity.<sup>18</sup> Unlike the Cys59 of SFGH, molecular modelling and mutation studies have revealed that this residue is very closely orientated with the catalytic triad, forming one side of the solvent-accessible surface of the S1 binding pocket.<sup>18</sup> As

**Figure 4.** Binding of product and tetrahedral intermediate to AtSFGH. (a) An AtSFGH subunit is shown binding the reaction product glutathione. (b) The interaction between glutathione and the active site residues at the molecular level. (c) The tetrahedral intermediate of S-acetylglutathione covalently bound to Ser152, as modelled by over-laying the active site of a PMSF-inhibited carboxylesterase from *Pseudomonas fluorescens*.

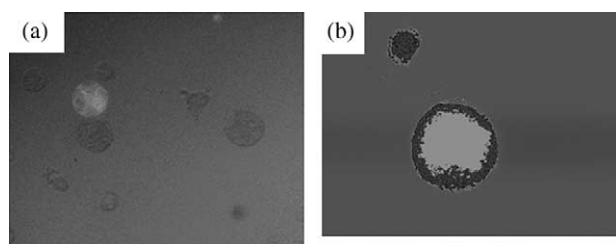


**Figure 5.** Regulation of *AtSFGH* by Cys59 *in vivo*. Fluorescence in protoplasts transfected with Cys59Ser mutant SFGH in the presence of 1 mM paraoxon. (a) An MUA-hydrolysing protoplast shown amongst inactive cells, with (b) a higher magnification image showing a single active cell adjacent to an inactive protoplast. No fluorescing protoplasts were observed following transfection with wild-type *AtSFGH* plasmid DNA.

such, the cysteine in carboxypeptidase Y participates directly in substrate binding as well as helping stabilize the tetrahedral intermediate of the transition state during catalysis. Similar dual roles for active site cysteine residues have been suggested by structural and mechanistic studies for other subtilisin-like serine hydrolases, such as the KEX2 protease (EC 3.4.21.61),<sup>19</sup> thermitase and proteinase K (3.4.21.64).<sup>20</sup> In each of these cases, the “regulatory” cysteine residue lies within 4–5 Å of essential catalytic residues and directly influences substrate binding and transition state formation. In contrast, the conserved cysteine residue in SFGHs is relatively distant (9 Å) from the catalytic residues and its exposed setting makes it very susceptible to alkylation and disulfide formation.

Since the gate-keeping cysteine is conserved completely in the SFGHs of bacteria, yeast, animals and plants, it is reasonable to assume that this residue has an important function in regulating the enzyme. The most logical explanation would be that under oxidising conditions, the regulatory cysteine inactivates SFGH, leading to a block in the hydrolysis of S-formylglutathione and hence formaldehyde detoxification. The purpose of such regulation is unclear, especially as the importance of the associated formaldehyde detoxification pathway is open to debate. In *E. coli*, the *frm* operon, which includes an *sfgH* gene, is strongly induced on exposure to formaldehyde, supporting a role for SFGH pathway in C-1 detoxification.<sup>9</sup> Similarly, formaldehyde is the primary oxidation product of methanol and essential roles for formaldehyde dehydrogenase and SFGH have been proposed in supporting methylotrophic growth in microorganisms. In *P. denitrificans*, SFGH was found to be essential for methylotrophic growth,<sup>6</sup> whereas both *C. boidinii*<sup>8</sup> and *S. cerevisiae*<sup>7</sup> continued to grow slowly in the presence of methanol and formaldehyde, respectively, on loss of their *sfgH* genes. In plants, although S-formylglutathione has been shown to be a metabolite of methanol,<sup>21</sup> a role for

SFGH in the formaldehyde detoxification pathway remains to be established.

While the functional significance of SFGH remains to be determined, the mechanism for its redox regulation can be proposed to be *via* disulfide formation of the regulatory cysteine with glutathione, which has precedence in the reversible inactivation of protein tyrosine phosphatases in plants and animals.<sup>23</sup> Our studies with the transient expression assays in the protoplasts revealed that the presence of the Cys59 led to the inactivation of the native *AtSFGH in vivo*. Due to the small numbers of cells transformed, it was not possible to determine how the introduced *AtSFGH* had been inactivated. However, we have recently carried out a proteomic screen for S-glutathionylated proteins in oxidatively stressed *Arabidopsis* cultured cells,<sup>23</sup> and a careful analysis of the lower-abundance polypeptides found to undergo mixed disulfide formation revealed the presence of *AtSFGH* (see Supplementary Data). This would suggest that *AtSFGH* becomes reversibly inactivated by S-glutathionylation in oxidatively stressed plant cells. Interestingly, since SFGH produces glutathione as a reaction product, it is probable that under oxidising conditions Cys59 would be particularly susceptible to S-glutathionylation as a by-product of catalysis, further pointing to the importance of this auto-regulatory mechanism. While strict on/off regulation of proteins by S-glutathionylation has precedence with the tyrosine phosphatases involved in redox sensing and signalling,<sup>22</sup> it is highly unusual for an enzyme with putative roles in primary metabolism.

In addition to the unusual regulation of the enzyme, SFGHs are interesting in being glutathione-dependent enzymes, which have evolved from the alpha-beta hydrolases, rather than the thioredoxin/glutaredoxin group of proteins.<sup>24</sup> The alpha-beta hydrolase family includes diverse enzymes, which are functionally accommodated by the insertion of polypeptide loops in the centre of the otherwise structurally conserved proteins. These loops can be of various sizes, ranging from just a few residues up to entire domains.<sup>25</sup> To understand how *AtSFGH* selectively binds glutathione thioesters, the structure of the *AtSFGH*-glutathione product complex was compared with that of a PMSF-inhibited carboxylesterase from *Pseudomonas fluorescens* (PDB ID 1AUR). When the structures of the two proteins were superimposed by modelling,<sup>26,27</sup> the active site residues (Ser152, Asp229 and His262) of *AtSFGH* were in very similar positions and orientations despite the low level of sequence homology (16% identity), as shown in Figure 4(c). This is true also for the backbone atoms of the residues forming the oxyanion hole, which by comparison were formed by the peptide nitrogen atoms of residues Met153 and Leu57 in *AtSFGH*. Using this overlay and with reference to the *AtSFGH*-glutathione molecular structure (Figure 4(b)), the tetrahedral intermediate of S-AG covalently bound at the active site could be

modelled (Figure 4(c)). We propose that the amino acids involved in coordinated substrate and product binding are His151, Tyr264, Lys67, Asn63, Asp261 and Gln230. Significantly, all these residues, with the exception of Gln230, are conserved in microbial, plant and mammalian SFGHs (Figure 1). In the model of the tetrahedral intermediate, His151 (adjacent to the catalytic serine), and Tyr264 interacted with the Gly of glutathione, whereas in the enzyme–product complex, Lys67 and the Asn63 assumed this role (Figure 4(b)). Additional interactions in the enzyme–product complex were observed between the Glu of glutathione and Gln230, which is next to the conserved aspartate of the catalytic triad, and Asp261, which is adjacent to the active site histidine residue. These active site amino acid residues are not seen in other plant alpha-beta hydrolases and help explain the unusual selectivity of *At*SFGH for glutathione thioesters.

The original classification of SFGH as an esterase D was due to the sensitivity of the enzyme to thiol-alkylating agents and its inability to either hydrolyse, or be inhibited by, organophosphate insecticides.<sup>4</sup> The conservation of the reactive and regulatory cysteine residue in SFGHs readily explains the sensitivity to sulfhydryl reagents. The explanation of the insensitivity of SFGHs to organophosphates lies in the topography of the active site. Thus, the overlay of the carboxylesterase shows that the approach of the bulky PMSF to the catalytic serine residue in *At*SFGH is blocked by Trp186 (Figure 4(c)). This steric hindrance would also explain why the similarly large paraoxon fails to inhibit the enzyme and now gives us a rational basis for describing this enzyme as a true serine hydrolase.

## Materials and Methods

### Substrates and protein modification agents.

S-Acetylglutathione<sup>10</sup> and FP-biotin<sup>13</sup> were synthesised using published procedures. MTS reagents (Figure 2) were prepared from the respective bromides.<sup>16</sup>

### *At*SFGH; expression, crystallization and structural determination

*At*SFGH was purified as its His-tagged fusion protein by Ni-chelate affinity chromatography.<sup>10</sup> For crystallization studies, the enzyme was also labelled with selenomethionine.<sup>12</sup> Pure proteins were analysed by SDS-PAGE and mass spectrometry prior to crystallization from 0.1 M imidazole-malate (pH 6.5), containing 0.2 M magnesium acetate, 16% (w/v) polyethylene glycol 4000 and 3% (v/v) methanol.<sup>12</sup> Crystals of selenomethionine (SeMet)-labelled protein were used to collect a multiwavelength anomalous diffraction (MAD) dataset at beamline BM14 of the European Synchrotron Radiation Facility (ERSF) and the data were collected and processed. Reflection data were indexed, integrated, and scaled using the HKL suite,<sup>28</sup> and phase determination was performed with the SOLVE program.<sup>29</sup> Phases were calculated on the three

**Table 2.** Data collection and refinement statistics

|  | <i>At</i> SFGH <sup>a</sup> | <i>At</i> SFGH/GSH complex |
|--|-----------------------------|----------------------------|
| <b>A. Data collection</b>                  |                             |                            |
| Space group                                | C2                          | C2                         |
| Cell dimensions                            |                             |                            |
| <i>a</i> (Å)                               | 128.6                       | 129.0                      |
| <i>b</i> (Å)                               | 80.8                        | 82.6                       |
| <i>c</i> (Å)                               | 93.9                        | 94.0                       |
| $\alpha$ (deg.)                            | 90                          | 90                         |
| $\beta$ (deg.)                             | 93.20                       | 93.6                       |
| $\gamma$ (deg.)                            | 90                          | 90                         |
| Resolution (Å)                             | 30–1.7 (1.76–1.7)           | 20–2.14 (2.22–2.14)        |
| $R_{\text{sym}}$ or $R_{\text{merge}}$ (%) | 6.9 (47.5)                  | 6.6 (41.3)                 |
| $I/\sigma$                                 | 22.4 (2.7)                  | 17.7 (2.7)                 |
| Completeness (%)                           | 99.3 (94.7)                 | 98.4 (96.8)                |
| Redundancy                                 | 5.6 (4.5)                   | 4.0 (3.6)                  |
| <b>B. Refinement</b>                       |                             |                            |
| Resolution (Å)                             | 1.7                         | 2.14                       |
| No. reflections                            | 99,218                      | 50,518                     |
| $R_{\text{work}}$ (%)                      | 18.2                        | 17.4                       |
| $R_{\text{free}}$ (%)                      | 21.5                        | 22.3                       |
| No. atoms                                  |                             |                            |
| Protein                                    | 6709                        | 6709                       |
| GSH  | –                           | 3                          |
| Water                                      | 547                         | 281                        |
| B-factors (Å <sup>2</sup> )                |                             |                            |
| Protein                                    | 19.7                        | 25.4                       |
| Ligand/ion                                 | –                           | 25.7                       |
| Water                                      | 24.2                        | 25.6                       |
| r.m.s deviations from ideal                |                             |                            |
| Bond lengths (Å)                           | 0.018                       | 0.015                      |
| Bond angles (deg.)                         | 1.5                         | 1.4                        |

Values in parentheses are for the outermost shell.

<sup>a</sup> Full statistics for the MAD data collection were as reported.<sup>12</sup>

wavelengths in the 30–2.3 Å resolution range and a solution was found using 12 selenium sites (mean figure of merit of 0.67 for all the data). The electron density map was improved by solvent flattening and phase extension to 1.7 Å resolution using DM (part of the CCP4 suite). An initial model was built using the program ARP/wARP<sup>30</sup> and completed and refined using the programs Xtal-View<sup>31</sup> and REFMAC5.<sup>32</sup> Non-crystallographic restraints were applied during refinement. A crystal of a Ser152Ala mutant of *At*SFGH was soaked in mother liquor containing 200 mM glutathione for two hours and then X-ray diffraction data were collected to 2.12 Å (Table 2). The structure of the *At*SFGH–glutathione complex was solved by molecular replacement using the native enzyme as a starting model, with refinement carried out as described above.

### Esterase assay and chemical inhibition treatments.

Hydrolase assays were performed with the carboxy-ester *p*NPA and the *S*-AG by spectrophotometry and with MUA by fluorimetry.<sup>10</sup> For inhibition studies, purified recombinant *At*SFGH (20 μM) was incubated in 10 mM ammonium acetate buffer (pH 7.4) with FP-biotin (25 μM–100 μM), iodoacetamide (1 mM–10 mM), or 1 mM *N*-ethylmaleimide for 30 min at 25 °C. *S*-Glutathionylation of *At*SFGH was performed by thiol exchange using oxidised glutathione.<sup>17</sup> For MTS-modification, *At*SFGH (20 μM) was incubated in 100 mM sodium phosphate (pH 7.2) containing 1.4 molar equivalents of each reagent for 30 min on ice. Proteins were desalted by gel-filtration before analysis.

## MS analysis

Protein masses were determined by ESI-TOF MS by direct infusion.<sup>17</sup> For HPLC-MS, polypeptides were injected onto a C18 column (150 mm × 2.4 mm, pore size 300 Å; Phenomenex) in water/acetonitrile (95:5, v/v) containing 0.5% (v/v) formic acid. Bound protein was eluted at 0.2 ml min<sup>-1</sup> with a linearly increasing gradient to 100% acetonitrile, 0.5% formic acid over 10 min. Protein spectra were deconvoluted using MaxEnt v 3.5 (Micro-mass) with reference to horse heart myoglobin. To identify residues undergoing covalent modification, derivatised proteins were desalted into 10 mM ammonium acetate (pH 7.4) and digested overnight at 37 °C in 50% (v/v) acetonitrile with sequencing-grade trypsin (Promega; molar ratio of protein to trypsin, 50:1). The digest was infused into the mass spectrometer in 0.5% (v/v) formic acid *via* a microsyringe and fused silica capillary at a flow rate of 10 µl min<sup>-1</sup>. Data were collected for 2 min in positive mode using sodium iodide and myoglobin for calibration, and summed to provide a total peptide mass spectrum over the range 100–2500 Da, with results compared to those obtained with native AtSFGH.

## Mutagenesis and protoplast expression studies with AtSFGH

PCR was used to generate the individual mutants Ser152Ala and Cys59Ser using the Quik-Change system (Stratagene). After confirming sequences, mutated plasmids were used to transform Rosetta DE3 pLysS cells (Novagen) for recombinant protein expression.<sup>10</sup> Native AtSFGH and mutant AtSFGHC59S were sub-cloned into the NcoI/KpnI sites of the plant expression vector pRT107, after using a custom oligonucleotide to introduce the KpnI site. *A. thaliana* (Ecoype Columbia) suspension cultures were grown to mid-logarithmic growth phase,<sup>23</sup> and used to prepare protoplasts in batches of 2 ml packed cell volume using a www protocol† as recently reviewed.<sup>33</sup> Following incubation, protoplasts were filtered through steel mesh (75 µm), pelleted (100 g, 2 min) and resuspended in 5 ml of W5 medium, (2 mM Mes (pH 5.7), 150 mM NaCl, 125 mM CaCl<sub>2</sub>, 5 mM KCl). After passing through 50 µm pore size filter units (DakoCytomation) protoplasts were repelleted, resuspended in W5 medium and then cell density was estimated using a haemocytometer. Protoplasts (10<sup>4</sup> in 100 µl) in 0.4 M mannitol, 15 mM MgCl<sub>2</sub>, were added to 10 µl of plasmid DNA (10 µg), followed by 110 µl of a solution containing 40% (w/v) PEG 4000, 0.2 M mannitol, 100 mM CaCl<sub>2</sub> and incubated at 23 °C for 15 min. Protoplasts were then diluted with 0.44 ml of W5 over 5 min, pelleted (100 g, 2 min) and resuspended in 1 ml of W5 prior to incubating at 23 °C overnight. To inhibit endogenous serine hydrolases, protoplasts were treated with 1 mM paraoxon for 30 min. Stock solutions (30 mM) of fluorescein diacetate and MUA in acetone were diluted 1:100 (v/v) with W5 medium (immediately prior to mixing 1:1 (v/v) with cells, which were then examined under a fluorescence microscope for viability (using fluorescein diacetate) and transgene expression (MUA).

† <http://genetics.mgh.harvard.edu/sheenweb/>

## Acknowledgements

This project received funding from the County Durham Sub Regional Partnership. R.E. acknowledges the support of a Research Development Fellowship awarded by the Biotechnology and Biological Sciences Research Council.

## Supplementary Data

Supplementary data associated with this article can be found, in the online version, at doi:10.1016/j.jmb.2006.03.048

## References

- Forouhar, F., Yang, Y., Kumar, D., Chen, Y., Fridman, E., Park, S. W. *et al.* (2005). Structural and biochemical studies identify tobacco SABP2 as a methyl salicylate esterase and implicate it in plant innate immunity. *Proc. Natl Acad. Sci USA*, **102**, 1773–1778.
- Ruppert, M., Ma, X. Y. & Stockigt, J. (2005). Alkaloid biosynthesis in *Rauvolfia*-cDNA cloning of major enzymes of the ajmaline pathway. *Curr. Org. Chem.* **95**, 1431–1444.
- Cummins, I. & Edwards, R. (2004). Purification and cloning of an esterase from the weed black-grass (*Alopecurus myosuroides*), which bioactivates aryloxyphenoxypropionate herbicides. *Plant J.* **39**, 894–904.
- Uotila, L. (1984). Polymorphism of red-cell S-formylglutathione hydrolase in a Finnish population. *Hum. Hered.* **34**, 273–277.
- Hanson, A. D., Gage, D. A. & Shachar-Hill, Y. (2000). Plant one-carbon metabolism and its engineering. *Trends Plant Sci.* **5**, 206–213.
- Harms, N., Ras, J., Reijnders, W. N. M., van Spanning, R. J. M. & Stouthamer, A. H. (1996). S-Formylglutathione hydrolase of *Paracoccus denitrificans* is homologous to human esterase D: a universal pathway for formaldehyde detoxification? *J. Bacteriol.* **178**, 6296–6299.
- Degrassi, G., Uotila, L., Klima, R. & Venturi, V. (1999). Purification and properties of an esterase from the yeast *Saccharomyces cerevisiae* and identification of the encoding gene. *Appl. Environ. Microbiol.* **65**, 3470–3472.
- Yurimoto, H., Lee, B., Yano, T., Sakai, Y. & Kato, N. (2003). Physiological role of S-formylglutathione hydrolase in C-1 metabolism of the methylotrophic yeast *Candida boidinii*. *Microbiol.-SGM*, **149**, 1971–1979.
- Herring, C. D. & Blattner, F. R. (2004). Global transcriptional effects of a suppressor tRNA and the inactivation of the regulator *frmR*. *J. Bacteriol.* **186**, 6714–6720.
- Kordic, S., Cummins, I. & Edwards, R. (2002). Cloning and characterization of a S-formylglutathione hydrolase from *Arabidopsis thaliana*. *Arch. Biochem. Biophys.* **399**, 232–238.
- Haslam, R., Rust, S., Pallett, K., Cole, D. & Coleman, J. (2002). Cloning and characterization of S-formylglutathione hydrolase from *Arabidopsis thaliana*: a pathway for formaldehyde detoxification. *J. Plant Physiol.* **40**, 281–288.
- McAuley, K. E., Cummins, I., Papiz, M., Edwards, R. & Fordham-Skelton, A. P. (2003). Purification, crystallisation and preliminary X-ray diffraction analysis of

- S-formylglutathione hydrolase from *Arabidopsis thaliana*: effects of pressure and selenomethionine substitution on space group changes. *Acta Crystallog. sect. D*, **59**, 2272–2274.
13. Liu, Y., Patricelli, M. P. & Cravatt, B. F. (1999). Activity-based protein profiling: the serine hydrolases. *Proc. Natl Acad. Sci. USA*, **96**, 14696–14699.
  14. Laskowski, R. A., MacArthur, M. W., Moss, D. S. & Thornton, J. M. (1993). PROCHECK: a program to check the stereochemical quality of protein structures. *J. Appl. Crystallog.* **26**, 283–291.
  15. Hooft, R. W. W., Vriend, G., Sander, C. & Abola, E. E. (1996). Errors in protein structures. *Nature*, **381**, 272.
  16. Berglund, P., DeSantis, G., Stabile, M. R., Shang, X., Gold, M., Bott, R. R. (1997). Chemical modification of cysteine mutants of subtilisin *Bacillus lentus* can create better catalysts than the wild-type enzyme. *J. Am. Chem. Soc.* **119**, 5265–5266.
  17. Dixon, D. P., Fordham-Skelton, A. P. & Edwards, R. (2005). Redox regulation of a soybean tyrosine-specific protein phosphatase. *Biochemistry*, **44**, 7696–7703.
  18. Mima, J., Jung, G., Onizuka, T., Ueno, H. & Hayashi, R. (2002). Amphipathic property of free thiol group contributes to an increase in the catalytic efficiency of carboxypeptidase Y. *Eur. J. Biochem.* **269**, 3220–3225.
  19. Holyoak, T., Wilson, M. A., Fenn, T. D., Kettner, C. A., Petsko, G. A., Fuller, R. S. & Ringe, D. (2003). Angstrom resolution crystal structure of the prototypical hormone-processing protease Kex2 in complex with an Ala-Lys-Arg boronic acid inhibitor. *Biochemistry*, **42**, 6709–6718.
  20. Jany, K. D., Lederer, G. & Mayer, B. (1986). Amino acid sequence of proteinase K from the mold *Trichothium album limber*—proteinase K, a subtilisin related enzyme with disulfide bonds. *FEBS Letters*, **199**, 139–144.
  21. Gout, E., Aubert, S., Bligny, R., Rebeille, F., Nonomura, A. R., Benson, A. A. & Douce, R. (2000). Metabolism of methanol in plant cells. Carbon-13 nuclear magnetic resonance studies. *Plant Physiol.* **123**, 287–296.
  22. Barrett, W. C., DeGnore, J. P., Konig, S., Fales, H. M., Keng, Y. F., Zhang, Z. Y. *et al.* (1999). Regulation of PTP1B via glutathionylation of the active site cysteine 215. *Biochemistry*, **38**, 6699–6705.
  23. Dixon, D. P., Skipsey, M., Grundy, N. M. & Edwards, R. (2005). Stress induced protein S-glutathionylation in *Arabidopsis thaliana*. *Plant Physiol.* **138**, 2233–2244.
  24. Martin, J. L. (1995). Thioredoxin—a fold for all reasons. *Structure*, **3**, 245–250.
  25. Nardini, M. & Dijkstra, B. W. (1999). Alpha/beta hydrolase fold enzymes: the family keeps growing. *Curr. Opin. Struct. Biol.* **9**, 732–737.
  26. Krissinel, E. & Henrick, K. (2004). Secondary-structure matching (SSM), a new tool for fast protein structure alignment in three dimensions. *Acta Crystallog. sect. D*, **60**, 2256–2268.
  27. Emsley, P. & Cowtan, K. (2004). Coot: model-building tools for molecular graphics. *Acta Crystallog. sect. D*, **60**, 2126–2132.
  28. Otwinowski, Z. & Minor, W. (1997). Processing of X-ray diffraction data collected in oscillation mode. *Methods Enzymol.* **276**, 307–326.
  29. Terwilliger, T. C. & Berendzen, J. (1999). Evaluation of macromolecular electron-density map quality using the correlation of local r.m.s. density. *Acta Crystallog. sect. D*, **55**, 849–861.
  30. Morris, R. J., Perrakis, A. & Lamzin, V. S. (2002). ARP/wARP's model-building algorithms. I. The main chain. *Acta Crystallog. sect. D*, **58**, 968–975.
  31. McRee, D. E. (1999). XtalView Xfit—a versatile program for manipulating atomic coordinates and electron density. *J. Struct. Biol.* **125**, 156–165.
  32. Murshudov, G. N., Vagin, A. A. & Dodson, E. J. (1997). Refinement of macromolecular structures by the maximum-likelihood method. *Acta. Crystallog. sect. D*, **53**, 240–255.
  33. Sheen, J. (2001). Signal transduction in maize and *Arabidopsis* mesophyll protoplasts. *Plant Physiol.* **127**, 1466–1475.
  34. DeLano, W. L. (2002). Unraveling hot spots in binding interfaces: progress and challenges. *Curr. Opin. Struct. Biol.* **12**, 14–20.

Edited by R. Huber

(Received 10 January 2006; received in revised form 17 March 2006; accepted 22 March 2006)  
Available online 3 April 2006